

UNVEILING FAR-INFRARED COUNTERPARTS OF BRIGHT SUBMILLIMETER GALAXIES USING PACS IMAGING

H. DANNERBAUER¹, E. DADDI¹, G. E. MORRISON^{2,3}, B. ALTIERI⁴, P. ANDREANI^{5,6}, H. AUSSSEL¹, S. BERTA⁷, A. BONGIOVANNI^{8,9}, A. CAVA^{8,9}, J. CEPAS^{8,9}, A. CIMATTI¹⁰, H. DOMINGUEZ¹¹, D. ELBAZ¹, N. FÖRSTER SCHREIBER⁷, R. GENZEL⁷, C. GRUPPIONI¹¹, B. HOREAU¹, H.S. HWANG¹, E. LE FLOC'H¹, J. LE PENNEC¹, D. LUTZ⁷, G. MAGDIS¹, B. MAGNELLI⁷, R. MAIOLINO¹², R. NORDON⁷, A.M. PÉREZ GARCÍA^{8,9}, A. POGELTSCH⁷, P. POPESSO⁷, F. POZZI¹⁰, L. RIGUCCINI¹, G. RODIGHIERO¹³, A. SAINTONGE⁷, P. SANTINI¹², M. SANCHEZ-PORTAL⁴, L. SHAO⁷, E. STURM⁷, L. TACCONI⁷, I. VALTCHANOV⁴

Draft version August 7, 2018

ABSTRACT

We present a search for Herschel-PACS counterparts of dust-obscured, high-redshift objects previously selected at submillimeter and millimeter wavelengths in the Great Observatories Origins Deep Survey North field. We detect 22 of 56 submillimeter galaxies (39%) with a SNR of ≥ 3 at 100 μm down to 3.0 mJy, and/or at 160 μm down to 5.7 mJy. The fraction of SMGs seen at 160 μm is higher than that at 100 μm . About 50% of radio-identified SMGs are associated with PACS sources. We find a trend between the SCUBA/PACS flux ratio and redshift, suggesting that these flux ratios could be used as a coarse redshift indicator. PACS undetected submm/mm selected sources tend to lie at higher redshifts than the PACS detected ones. A total of 12 sources (21% of our SMG sample) remain unidentified and the fact that they are blank fields at Herschel-PACS and VLA 20 cm wavelength may imply higher redshifts for them than for the average SMG population (e.g., $z > 3 - 4$). The Herschel-PACS imaging of these dust-obscured starbursts at high-redshifts suggests that their far-infrared spectral energy distributions have significantly different shapes than template libraries of local infrared galaxies.

Subject headings: Galaxies: high-redshift — Galaxies: individual (GN13 alias HDF850.4) — Galaxies: starburst — Cosmology: observations — Infrared: Galaxies — Submillimeter: galaxies

1. INTRODUCTION

Several hundred dust-enshrouded high- z sources have been selected through submm/mm imaging with bolometer cameras like SCUBA, LABOCA, AzTEC, MAMBO (e.g., Bertoldi et al. 2007; Coppin et al. 2006; Dannerbauer et al. 2002, 2004; Hughes et al. 1998; Perera et al. 2008; Pope et al. 2006; Smail et al. 2002; Weiß et al. 2009). The large beam size in the (sub)millimeter (e.g., MAMBO: 11"; SCUBA: 15"; LABOCA: 19") hampers the identification of these so-called Submillimeter Galaxies (SMGs; see

for a review Blain et al. 2002) based on bolometer data only. The most obvious choice for obtaining the subarcsecond accurate positions of the dust continuum is (sub)millimeter interferometric continuum observations (e.g., Dannerbauer et al. 2002, 2008; Younger et al. 2007). However the slow mapping speed of (sub)millimeter interferometers does not allow us to study a large number of sources. The most suitable tool for counterpart identification is interferometric observations at radio wavelengths. About 50% – 80% of these submm/mm sources have been identified, mainly based on radio observations, and the peak of the redshift distribution of the radio-identified SMG population lies at $\langle z \rangle = 2.2$ (Chapman et al. 2005). However, the effect of the bias toward the true redshift distribution introduced by the radio selection technique is still under debate, as SMGs even beyond $z = 4$ have been already detected by the VLA at 20 cm (e.g., Capak et al. 2008; Coppin et al. 2009; Daddi et al. 2009a,b; Knudsen et al. 2010; Morrison et al. 2010; Schinnerer et al. 2008). The sample of unidentified SMGs could be either spurious sources or lie at extreme redshifts but no systematic studies on this subsample of SMGs have been conducted so far.

The launch of the Herschel observatory (Pilbratt et al. 2010) promises a different perspective of SMGs than provided by radio observations only and offers a higher mapping speed than (sub)mm interferometric observations. Deep PACS (Pogelt et al. 2010) imaging at 100 μm and 160 μm on the Great Observatories Origins Deep Survey North (GOODS-N) will sample the FIR

¹ Laboratoire AIM, CEA/DSM - CNRS - Université Paris Diderot, DAPNIA/Service d'Astrophysique, CEA Saclay, Orme des Merisiers, F-91191 Gif-sur-Yvette Cedex, France

² Institute for Astronomy, University of Hawaii, Manoa, Hawaii 96822, USA

³ Canada-France-Hawaii Telescope Corp., Kamuela, Hawaii 96743, USA

⁴ Herschel Science Centre

⁵ ESO, Karl-Schwarzschild-Str. 2, D-85748 Garching, Germany

⁶ INAF - Osservatorio Astronomico di Trieste, via Tiepolo 11, 34143 Trieste, Italy

⁷ Max-Planck-Institut für Extraterrestrische Physik (MPE), Postfach 1312, 85741 Garching, Germany

⁸ Instituto de Astrofísica de Canarias, 38205 La Laguna, Spain

⁹ Departamento de Astrofísica, Universidad de La Laguna, Spain

¹⁰ Dipartimento di Astronomia, Università di Bologna, Via Ranzani 1, 40127 Bologna, Italy

¹¹ INAF-Osservatorio Astronomico di Bologna, via Ranzani 1, I-40127 Bologna, Italy

¹² INAF - Osservatorio Astronomico di Roma, via di Frascati 33, 00040 Monte Porzio Catone, Italy

¹³ Dipartimento di Astronomia, Università di Padova, Vicolo dell'Osservatorio 3, 35122 Padova, Italy

emission of these dust-enshrouded high- z objects and enable us to study in detail their far-infrared spectral energy distribution (SED), redshift distribution, dust temperatures (Chenial et al. 2010; Elbaz et al. 2010; Magnelli et al. 2010) and dust masses (Santini et al. 2010). In absence of interferometric observations at mm and cm wavelengths, the Herschel-PACS beamsize at $100\ \mu\text{m}$ ($160\ \mu\text{m}$) of $6.7''$ ($11.0''$) provide a more accurate location of the dust emission than the bolometer data taken with SCUBA, AzTEC, MAMBO or LABOCA.

In this letter we discuss our search for PACS counterparts at $100\ \mu\text{m}$ and $160\ \mu\text{m}$, explore the diagnostic potential of Herschel-PACS for the counterpart identification and compare it with the widely used identification approach using VLA observations. In comparison, the Spitzer-MIPS $70\ \mu\text{m}$ and $160\ \mu\text{m}$ imaging of the GOODS North region performed by Huynh et al. (2007) in the pre-Herschel era detected at relatively high significance only two (one) out of 30 SMGs at $70\ \mu\text{m}$ ($160\ \mu\text{m}$), at rather low redshifts ($z = 0.5$ and $z = 1.2$). The FIR observations presented here will enable us to study a significant sample of SMGs in the far-infrared wavelength regime.

2. FAR-INFRARED ASSOCIATION OF SUBMILLIMETER GALAXIES

PACS observations of the GOODS North region at $100\ \mu\text{m}$ and $160\ \mu\text{m}$ were taken during the Herschel Science Demonstration Phase in autumn 2009 and are part of the Guarantee Time extragalactic PACS survey ‘PEP: The PACS Evolutionary Probe’ (PI: D. Lutz). The final images achieve 3σ sensitivities of $\sim 3.0\ \text{mJy}$ and $\sim 5.7\ \text{mJy}$ at $100\ \mu\text{m}$ and $160\ \mu\text{m}$ respectively. Berta et al. (2010) describe in their appendix the Herschel-PACS observations, data reduction and the blind extraction of PACS sources with $\text{SNR} \geq 3$. Lutz et al. (in prep.) will present the fluxes of PACS sources. The PACS images are aligned on the GOODS imaging products. Complementary to the Herschel PACS observations, we use for this work data from the VLA at $1.4\ \text{GHz}$ (Morrison et al. 2010) and Spitzer-MIPS at $24\ \mu\text{m}$ (Dickinson et al., in prep.).

In the past years, several groups surveyed the GOODS North region using the bolometer cameras SCUBA, AzTEC and MAMBO (Borys et al. 2003; Greve et al. 2008; Hughes et al. 1998; Perera et al. 2008; Pope et al. 2005; Wang et al. 2004). These observations discovered about 150 SMGs at $850\ \mu\text{m}$, 1.1 and $1.2\ \text{mm}$. Robustly identified VLA and MIPS $24\ \mu\text{m}$ counterparts are already known in the literature for SCUBA and AzTEC sources (Chapin et al. 2009; Pope et al. 2006). In addition, Greve et al. (2008) presented VLA counterparts for 11 out of 30 MAMBO sources.

We search for Herschel-PACS counterparts of SMGs that are either detected with a SNR of ≥ 4 or detected by at least two different surveys. 56 SMGs fulfill this criterion which should assure a robust SMG sample to work with. Our sample¹⁴ consists of 36 SCUBA, 12 AzTEC and 8 MAMBO sources and for 15 SMGs

¹⁴ In case that an SMG is detected at submm and mm bands, we give preference the SCUBA detection and include it in our sample. For mm-only detected sources we list, if available, the AzTEC otherwise the MAMBO detection.

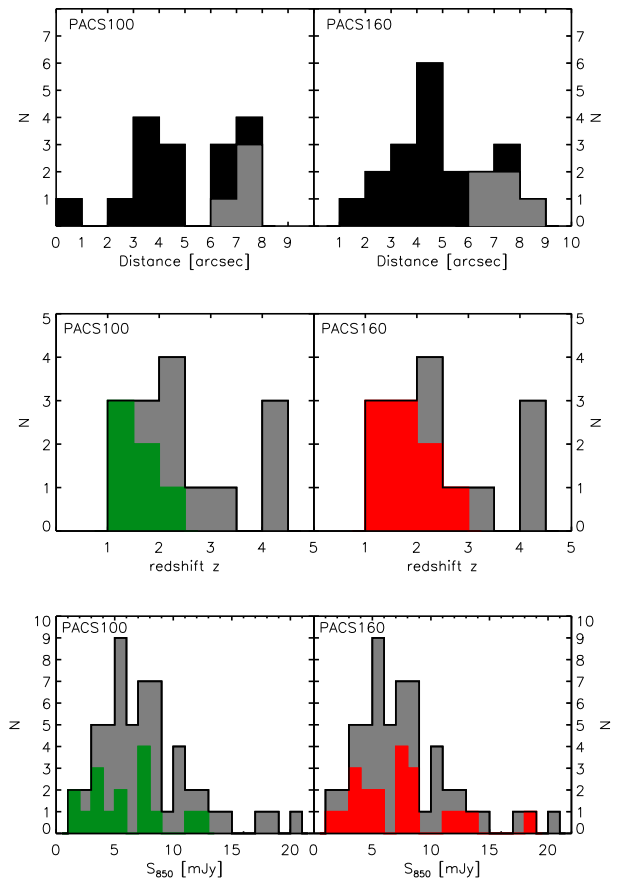


FIG. 1.— *Top panel:* Histogram of distance between the submm/mm position from the bolometric map and PACS positions of associated FIR sources at $100\ \mu\text{m}$ (left) and $160\ \mu\text{m}$ (right). Black and gray indicate secure and possible PACS counterparts. *Middle panel:* We show the redshift distribution for our SMG sample with spectroscopic redshifts (gray) and overplot our PACS detections at $100\ \mu\text{m}$ (green) respectively $160\ \mu\text{m}$ (red). *Lower panel:* We show the SCUBA flux distribution of our SMG sample (gray) and overplot our PACS detections at $100\ \mu\text{m}$ (green) respectively $160\ \mu\text{m}$ (red).

spectroscopic redshifts (SMG_{spec}) have been already obtained. We match our SMG sample with the PACS $100\ \mu\text{m}$ and $160\ \mu\text{m}$ blind catalogue and search for counterparts within a radius of $5.5''$ for MAMBO sources, $7.5''$ for SCUBA sources and $9''$ for AzTEC sources. As a sanity check of the blind catalogue, we inspected by eye the search region in the PACS imaging. The search circles that we have applied correspond to the beam size (FWHM) of the different bolometric datasets and should guarantee that no reliable associations to SMGs will be missed. We also searched the VLA $1.4\ \text{GHz}$ map and the MIPS $24\ \mu\text{m}$ images for counterparts at the SMG positions.

We calculate the corrected Poissonian probability p that an association of SMGs within the search radius is a chance coincidence. This approach (see for details Downes et al. 1986) corrects the simple Poissonian probability of a detected association for the possibility of associations of different nature but similar probability. The derived probability of PACS and MIPS association is based on raw number counts in GOODS North. We

search for VLA counterparts of SMGs down to 3σ . However, the VLA source catalogue (Morrison et al. 2010) is only reliable down to $20 \mu\text{Jy}$ ($\sim 5\sigma$). Therefore, we assess the reliability of VLA counterparts relying on published number counts (e.g., Fomalont et al. 2006). Similar to previous studies, we define following quality criteria for assessing the robustness of identified candidate counterparts. We classify association of SMGs with $p \leq 0.05$ as secure and with $0.05 < p \leq 0.10$ as possible counterparts.

We uncover PACS secure or possible counterparts for 22 SMGs, corresponding to a PACS identification rate of 39% of our whole SMG sample, see also Table 1 for details. Our PACS identification rate of 39% is lower than the rate of 54% found by Magnelli et al. (2010). The reason is that Magnelli et al. (2010) focus on already radio-identified SCUBA and AzTEC sources with spectroscopic redshifts mainly. The top panel of Fig. 1 displays the (sub)millimeter-PACS separation of our association. We did not find evidence of systematic offsets. We find PACS counterparts at a mean (sub)millimeter-PACS positional offset of $\Delta_{(\text{submm})\text{mm}-\text{PACS}100} = 5.0'' \pm 2.1''$ and $\Delta_{(\text{submm})\text{mm}-\text{PACS}160} = 4.9'' \pm 2.0''$. This is consistent with a typical submm/mm position error of about $3''$ to $5''$ and strengthens our choice of the FWHM of the bolometric data as search circle for PACS counterparts. The top panel of Fig. 1 shows clearly a dominance of secure counterparts. Given this statistical approach, associations with offsets much larger than the average might not always be correct.

TABLE 1
PACS ASSOCIATIONS OF 56 SUBMILLIMETER GALAXIES IN GOODS-N

	PACS 100 μm	PACS 160 μm
# secure association	12	15
# possible association	4	5
total identification rate	28.6%	35.7%
(sub)mm-PACS offset	$5.0'' \pm 2.1''$	$4.9'' \pm 2.0''$
	PACS 100 + 160 μm	
# total association of SMGs	22 (39.3%)	
# only detected at PACS 160 μm	6	
# only detected at PACS 100 μm	2	
new CPTs identified by PACS	1	
# PACS and radio blank fields	12 (21.4%)	

We detect 20 (16) SMGs at 160 (100) μm and classify 15 (12) of them as secure and 5 (4) as possible counterparts. The number of PACS counterparts at 160 μm is higher than at 100 μm . This is expected as the 160 μm measurements lie close to the FIR peak. We note that based on the corrected Poissonian probability p each PACS detection within the bolometer beam (our search circle) is classified as associated SMG counterpart. Typical PACS fluxes of these dust-obscured high- z sources range between 4.0 mJy to 34.9 mJy at 100 μm and 5.0 mJy to 65.0 mJy at 160 μm .

We have 43 (28 are secure; 15 are possible) radio-identified SMGs in our sample, about 50% of them are seen at PACS wavelengths. Vice-versa, only one PACS association (secure) is undetected at 1.4 GHz, see detailed discussion of GN13 (alias HDF850.4) at end of Section 3. One-third of PACS detected SMGs have at

least two VLA counterparts.

3. DIAGNOSTIC POTENTIAL OF PACS OBSERVATIONS OF SUBMILLIMETER GALAXIES

About twice as many SMGs are identified by the VLA than by PACS. VLA observations are more sensitive for sources at redshifts up to $z = 4$. None of the well-known, spectroscopically identified SMGs at $z = 4$ — GN20, GN20.2a/b and GN10 (Daddi et al. 2009a,b; Dannerbauer et al. 2008; Wang et al. 2007, 2009) — have been significantly detected in our PACS imaging, see middle panel in Fig. 1. Another highly promising $z \geq 4$ candidate, HDF850.1 (Cowie et al. 2009; Dunlop et al. 2004; Hughes et al. 1998) is also not seen by PACS. However, all these SMGs have radio counterparts. Focusing on our spectroscopic subsample of 15 sources, SMG_{spec} , we find a trend that the fraction of SMGs detected at PACS bands decreases with redshift (see middle panel in Fig. 1), being explained by the fact that PACS fluxes drop with increasing redshift. No source beyond $z = 2.00$ (GN06) at 100 μm and $z = 2.58$ (GN04) at 160 μm is significantly detected by PACS. However, we do not find evidence that the PACS detection rate of SMGs correlates with the SCUBA flux density (Fig. 1). In addition, VLA observations provide subarcsecond accurate positions which are essential for the proper identification in the optical and near-infrared bands and follow-up spectroscopic observations. PACS cannot deliver positions at these accuracies. To summarize, ultra-deep VLA observations still remain the best and most effective approach to identify SMG counterparts, even up to redshift $z = 4$.

Using only radio, 850 μm and 24 μm flux densities, Daddi et al. (2009a) derived accurate ($\Delta z / (1+z) \sim 0.1$) radio-IR photometric redshifts for SMGs. Motivated by this work, we apply the radio-IR photometric redshift code presented in Daddi et al. (2009a) and calculate photometric redshifts by adding our PACS measurements to existing SCUBA, MIPS 24 μm and VLA 1.4 GHz flux measurements of our SMG sample. Naively we would have expected to improve the accuracy of the radio-IR photometric redshifts by adding FIR measurements shortwards to the IR dust peak. In Fig. 2 we show the results of our attempt using template libraries of local galaxies (Chary & Elbaz 2001). In the left panel we show photometric redshifts (adapted from Daddi et al. 2009a) based on radio, MIR and submm observations for SCUBA counterparts with known spectroscopic redshifts in GOODS North which agree fairly well. In the right panel we show photometric redshift estimates adding the PACS measurements to our previous measurements in the radio, MIR and submm. Clearly the obtained accuracy decreases and these photo- z estimates are poorer. Omitting certain measurements (e.g., MIPS 24 μm and/or VLA 1.4 GHz) gives even worse results. We obtain similar results by using template libraries from Dale & Helou (2002) and the average SED constructed by Michałowski et al. (2010) of 73 spectroscopically identified SMGs (Chapman et al. 2005). This result means that most likely the far-infrared properties of SMGs are different from templates built to describe local galaxies. These observed differences arise most probably from the fact that SMGs are colder than local ULIRGs of same luminosity (Chanial et al. 2010; Chapman et al. 2005; Elbaz et al. 2010; Magnelli et al.

2010). Further investigations are needed to fully exploit the Herschel-PACS imaging in order to obtain accurate photometric redshifts.

We already know the spectroscopic redshift for 15 SMGs in our sample. However, in absence of spectroscopic redshifts for most of our sources, searching for correlations between observed properties is essential for constraining the nature, redshift and evolution of SMGs. We explore if flux ratios involving PACS 100 μm and 160 μm measurements can be used as a rough redshift indicator. Fig. 3 displays the results of our analysis. The PACS color ($S_{160\ \mu\text{m}}/S_{100\ \mu\text{m}}$) of SMGs does not vary with redshift and is consistent with the prediction of models and observed SEDs from Chary & Elbaz (2001), Michałowski et al. (2010), Armus et al. (2007) and Pope et al. (2008). The PACS colors seem to be slightly redder than predicted by the various models and may indicate a difference between the observed FIR-SED of SMGs and templates describing fairly well local infrared galaxies. The composite rest-frame SED for the SMG_{spec} (Fig. 3) subsample shows their diversity in the far-infrared. Their far-infrared colors are different from the template SEDs, most notably for the local luminous infrared galaxies. This may explain our finding reported above that we are not able to obtain accurate IR-radio photometric redshifts by including PACS measurements.

The PACS fluxes are redshift dependent, whereas the (sub)millimeter flux density at $z \geq 1$ is not (due to the negative K-correction; e.g., Blain et al. 2002), thus one would expect to see a trend between (sub)mm/PACS flux ratio for both PACS bands (see also the predictions based on different templates in Fig. 3). Indeed, we find a fairly clear trend both for $S_{850\ \mu\text{m}}/S_{160\ \mu\text{m}}$ respectively $S_{850\ \mu\text{m}}/S_{100\ \mu\text{m}}$ versus spectroscopic redshift for the SMG_{spec} subsample¹⁵ over the whole redshift range spanned by our SMGs from $z \sim 1 - 4$. We conclude that the (sub)mm/PACS flux ratio seems to be a useful albeit crude redshift indicator and may help to se-

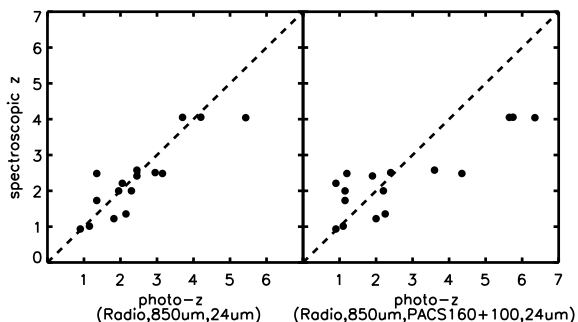


FIG. 2.— Comparison of spectroscopic and photometric redshifts. In the left panel we show photometric redshifts based on radio, 850 μm and 24 μm flux densities measurements for SMG counterparts with spectroscopic redshifts in GOODS North (adopted from Daddi et al. 2009a). There is a fairly good agreement. In the right panel, we show photometric redshift estimates including PACS measurements which are less reliable.

¹⁵ For SCUBA sources from Pope et al. (2006) we use the de-boosted flux. The same we do for AzTEC and MAMBO sources. We converted the AzTEC and MAMBO mm flux densities into SCUBA flux densities by assuming a flux ratio of $S_{850}/S_{1\ \text{mm}}$ of 2.5 for a ULIRG-like SED at redshift $z \sim 2 - 3$.

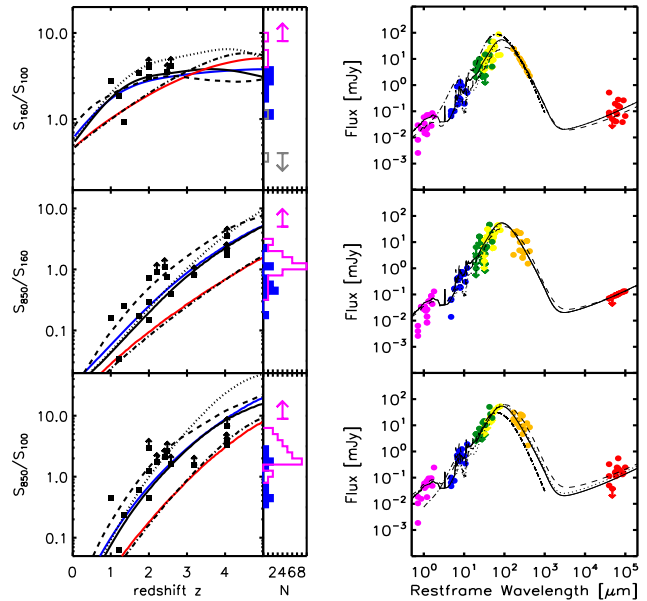


FIG. 3.— *Left Panels:* From top to bottom we plot the flux ratios $S_{160\ \mu\text{m}}/S_{100\ \mu\text{m}}$, $S_{850\ \mu\text{m}}/S_{160\ \mu\text{m}}$ and $S_{850\ \mu\text{m}}/S_{100\ \mu\text{m}}$ versus redshift for SMGs with spectroscopic redshifts. Template SEDs of a local LIRG with $L_{\text{IR}} \approx 1 \times 10^{11} L_{\odot}$ (blue-solid line), a local ULIRG with $L_{\text{IR}} \approx 1 \times 10^{12} L_{\odot}$ (black-solid line) and a HyLIRG with $L_{\text{IR}} \approx 1 \times 10^{13} L_{\odot}$ (red-solid line), all from Chary & Elbaz (2001), and an average SMG (black-dashed line, Michałowski et al. 2010), are shown for comparison. Average SEDs including Spitzer-IRS spectroscopy of local ULIRGs (black-dashed-dotted line, Armus et al. 2007) and SMGs (black-dotted line, Pope et al. 2008) are shown as well. The histograms present the distribution of SMGs without spectroscopic redshifts (blue-filled), lower limits of flux ratios are displayed by the pink-empty histogram. For the $S_{160\ \mu\text{m}}/S_{100\ \mu\text{m}}$ flux ratio we show the upper limit as gray-empty histogram. The pink (gray) arrow underlines the limits. *Right Panels:* From top to bottom, we plot the composite rest-frame SED — IRAC 3.6 μm (pink), MIPS 24 μm (blue), PACS 100 μm (green), PACS 160 μm (green), SCUBA 850 μm (gold), VLA 20 cm (red) — of our spectroscopic SMG sample normalized on SCUBA, VLA and PACS 160 μm fluxes. Template SEDs of ULIRGs and SMGs are shown for comparison. Both data points and templates are normalized on an SMG with a SCUBA flux of 8 mJy at $z = 2.2$.

lect/mark SMGs at very high-redshifts. We explored also VLA/PACS and PACS/MIPS 24 μm flux ratios versus redshift but did not observe any correlation, being consistent with the fact that VLA, MIPS 24 μm and PACS fluxes drop with increasing redshift. Based on this finding, we investigate the (sub)mm/PACS ratio for the remaining 41 SMGs without any reliable redshift. This analysis shows that PACS-detected SMGs tend to have lower flux ratios than the PACS-undetected SMG sample (Fig. 3). This trend seems to be more prominent for the $S_{850\ \mu\text{m}}/S_{160\ \mu\text{m}}$ flux density ratio. Our analysis may indicate that indeed as previously discussed PACS-undetected SMGs could tend to lie at higher redshifts and the (sub)mm/PACS flux ratio could be a crucial tool to select the very high- z tail of the SMG population.

The previous analysis bridges with the discovery that 12 out of 56 SMGs (21%) in our sample are blank fields both at PACS and radio wavelengths. The nature of these sources is still not clear. These SMGs could be either spurious sources which is mainly assumed, or at redshifts higher than $z > 4$. Indeed, how reliable are these

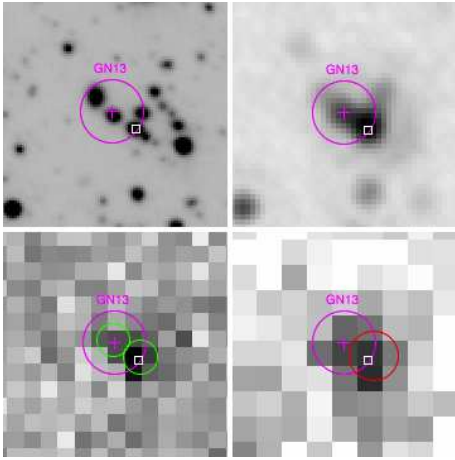


FIG. 4.— From left to right and top to bottom we show the $50'' \times 50''$ IRAC $3.6\mu\text{m}$, MIPS $24\mu\text{m}$, PACS $100\mu\text{m}$ and PACS $160\mu\text{m}$ images of the field of GN13 alias HDF850.4 (Hughes et al. 1998; Pope et al. 2006), north is up and east to the left. The $7.5''$ search radius circle at the nominal SCUBA position of GN13 (magenta cross) is drawn. Green (red) circles represent PACS $100\mu\text{m}$ (PACS $160\mu\text{m}$) $\geq 3\sigma$ detections and the white square a VLA source. Daddi et al. (2009a) suggested that the counterpart at $z = 0.457$ in South-West direction $\sim 7''$ away from GN13 is a mis-identification. We propose the PACS $100\mu\text{m}$ detection on top of the nominal SCUBA position (magenta cross) as new counterpart at $z \sim 1 - 2.5$.

(sub)mm sources detections? The sample consists of seven submillimeter and five millimeter selected sources (of the latter population, one is seen by AzTEC and four by MAMBO). We checked each source for its reliability. The mm sources are selected with $\text{SNR} \geq 4$. Four of the seven SCUBA galaxies are listed in both Pope et al. (2006) and Wang et al. (2004). The fact that Pope et al. (2006) and Wang et al. (2004) used (nearly) the same SCUBA data, but performed independent data reduction and source extraction, is giving more weight to the reliability of these detections. As a sanity check we inspected

the SCUBA and MAMBO galaxies in the AzTEC 1mm map. Our analysis suggests that most of these sources are reliable. One of them has a $\text{SNR} \sim 9$ at $850\mu\text{m}$. However, we note that only mm interferometric observations will reveal unambiguously the reliability of these sources. Their non-detection both at radio and PACS wavebands in combination with its (sub)mm/PACS flux ratio may suggest that these sources could lie at higher redshifts than the typical SMG population (e.g., $z > 3 - 4$).

We conclude this work by presenting the identification of an SMG counterpart having a PACS but no VLA detection. Daddi et al. (2009a) suspected that the source at $z_{\text{spec}} = 0.457$, about $7''$ away from the SCUBA position, could not be the correct counterpart of GN13 alias HDF850.4 (Hughes et al. 1998; Pope et al. 2006). We detect a faint (4.2σ), secure counterpart at $100\mu\text{m}$, being very close to the bolometer position ($\sim 0.6''$). Its reliability is fortified by a $200\mu\text{Jy}$ strong, secure counterpart at $24\mu\text{m}$. Using the flux ratios $S_{850\mu\text{m}}/S_{100\mu\text{m}} = 0.38$ and $S_{850\mu\text{m}}/S_{160\mu\text{m}} > 0.37$ as a coarse redshift indicator suggests a redshift of $z \sim 1 - 2.5$.

PACS has been developed by a consortium of institutes led by MPE (Germany) and including UVIE (Austria); KUL, CSL, IMEC (Belgium); CEA, OAMP (France); MPIA (Germany); IFSI, OAP/OAT, OAA/CAISMI, LENS, SISSA (Italy); IAC (Spain). This development has been supported by the funding agencies BMVIT (Austria), ESA-PRODEX (Belgium), CEA/CNES (France), DLR (Germany), ASI (Italy), and CICYT/MCYT (Spain). We thank Alex Pope and Lee Armus for providing SEDs of SMGs and local ULIRGs. We thank an anonymous referee for useful comments that improved our manuscript. We acknowledge the funding support of the ERC-StG grant UPGAL 240039 and ANR-08-JCJC-0008.

REFERENCES

- Armus, L., et al. 2007, *ApJ*, 656, 148
 Berta, S., et al. 2010, *A&A*, in press (astro-ph/1005.1073)
 Bertoldi, F., et al. 2007, *ApJS*, 172, 132
 Blain, A. W., Smail, I., Ivison, R. J., Kneib, J.-P., & Frayer, D. T. 2002, *Phys. Rep.*, 369, 111
 Borys, C., Chapman, S., Halpern, M., & Scott, D. 2003, *MNRAS*, 344, 385
 Capak, P., et al. 2008, *ApJ*, 681, L53
 Chanial, P., et al. 2010, in preparation
 Chapin, E. L., et al. 2009, *MNRAS*, 398, 1793
 Chapman, S. C., Blain, A. W., Smail, I., & Ivison, R. J. 2005, *ApJ*, 622, 772
 Chary, R., & Elbaz, D. 2001, *ApJ*, 556, 562
 Coppin, K., et al. 2006, *MNRAS*, 372, 1621
 Coppin, K. E. K., et al. 2009, *MNRAS*, 395, 1905
 Cowie, L. L., Barger, A. J., Wang, W.-H., & Williams, J. P. 2009, *ApJ*, 697, L122
 Daddi, E., et al. 2009a, *ApJ*, 694, 1517
 Daddi, E., Dannerbauer, H., Krips, M., Walter, F., Dickinson, M., Elbaz, D., & Morrison, G. E. 2009b, *ApJ*, 695, L176
 Dale, D. A., & Helou, G. 2002, *ApJ*, 576, 159
 Dannerbauer, H., Lehnert, M. D., Lutz, D., Tacconi, L., Bertoldi, F., Carilli, C., Genzel, R., & Menten, K. 2002, *ApJ*, 573, 473
 Dannerbauer, H., Lehnert, M. D., Lutz, D., Tacconi, L., Bertoldi, F., Carilli, C., Genzel, R., & Menten, K. M. 2004, *ApJ*, 606, 664
 Dannerbauer, H., Walter, F., & Morrison, G. 2008, *ApJ*, 673, L127
 Downes, A. J. B., Peacock, J. A., Savage, A., & Carrie, D. R. 1986, *MNRAS*, 218, 31
 Dunlop, J. S., et al. 2004, *MNRAS*, 350, 769
 Elbaz, D., et al. 2010, *A&A*, in press (astro-ph/1005.2859)
 Fomalont, E. B., Kellermann, K. I., Cowie, L. L., Capak, P., Barger, A. J., Partridge, R. B., Windhorst, R. A., & Richards, E. A. 2006, *ApJS*, 167, 103
 Greve, T. R., Pope, A., Scott, D., Ivison, R. J., Borys, C., Conselice, C. J., & Bertoldi, F. 2008, *MNRAS*, 389, 1489
 Hughes, D. H., et al. 1998, *Nature*, 394, 241
 Huynh, M. T., Pope, A., Frayer, D. T., & Scott, D. 2007, *ApJ*, 659, 305
 Knudsen, K. K., Kneib, J.-P., Richard, J., Petitpas, G., & Egami, E. 2010, *ApJ*, 709, 210
 Magnelli, B., et al. 2010, *A&A*, in press (astro-ph/1005.1154)
 Michałowski, M. J., Hjorth, J., & Watson, D. 2010, *A&A*, in press (astro-ph/0905.4499)
 Morrison, G. E., Owen, F. N., Dickinson, M., Ivison, R. J., & Ibar, E., 2010, *ApJS*, 188, 178
 Perera, T. A., et al. 2008, *MNRAS*, 391, 1227
 Pilbratt, G., et al. 2010, *A&A*, in press (astro-ph/1005.5331)
 Poglitsch, A., et al. 2010, *A&A*, in press (astro-ph/1005.1487)
 Pope, A., Borys, C., Scott, D., Conselice, C., Dickinson, M., & Mobasher, B. 2005, *MNRAS*, 358, 149
 Pope, A., et al. 2006, *MNRAS*, 370, 1185
 Pope, A., et al. 2008, *ApJ*, 675, 1171
 Santini, P., et al. 2010, *A&A*, in press (astro-ph/1005.5678)

- Schinnerer, E., et al. 2008, ApJ, 689, L5
Smail, I., Ivison, R. J., & Blain, A. W. 1997, ApJ, 490, L5
Smail, I., Ivison, R. J., Blain, A. W., & Kneib, J.-P. 2002, MNRAS, 331, 495
Wang, W.-H., Cowie, L. L., & Barger, A. J. 2004, ApJ, 613, 655
Wang, W.-H., Cowie, L. L., van Saders, J., Barger, A. J., & Williams, J. P. 2007, ApJ, 670, L89
Wang, W.-H., Barger, A. J., & Cowie, L. L. 2009, ApJ, 690, 319
Weiß, A., et al. 2009, ApJ, 707, 1201
Younger, J. D., et al. 2007, ApJ, 671, 1531